Quantum Computing for Molecular Energy Simulations

Quantum Computation for Molecular Energy Simulations

James D. Whitfield[a], Jacob Biamonte[a,b], and Alán Aspuru-Guzik[a]*

[a] *Harvard University, Department of Chemistry and Chemical Biology, 12 Oxford St., Cambridge, MA, 02138, USA*;

[b] *Oxford University Computing Laboratory, Oxford OX1 3QD, UK*

()

Over the last century, a large number of physical and mathematical developments paired with rapidly advancing technology have allowed the field of quantum chemistry to advance dramatically. However, the lack of computationally efficient methods for the exact simulation of quantum systems on classical computers presents a limitation of current computational approaches. We report, in detail, how a set of pre-computed molecular integrals can be used to explicitly create a quantum circuit, i.e. a sequence of elementary quantum operations, that, when run on a quantum computer, to obtain the energy of a molecular system with fixed nuclear geometry using the quantum phase estimation algorithm. We extend several known results related to this idea and discuss the adiabatic state preparation procedure for preparing the input states used in the algorithm. With current and near future quantum devices in mind, we provide a complete example using the hydrogen molecule, of how a chemical Hamiltonian can be simulated using a quantum computer.

Keywords: electronic structure, quantum computing

1. Introduction

Theoretical and computational chemistry involves solving the equations of motion that govern quantum systems by analytical and numerical methods [1, 2]. Except in standard cases such as, the harmonic oscillator or the hydrogen atom, analytic solutions are not known and computational methods have been developed.

Although classical computers have tremendously aided our understanding of chemical systems and their processes, the computational cost of the numerical methods for solving Schrödinger's equation grows rapidly with increases in the quality of the description. Research is ongoing to improve computational methods, but large molecules and large basis sets have remained a consistent problem despite the exponential growth of computational power of classical computers [3].

Theoretical computer science suggests that these limitations are not mere shortcomings of the programmers but could stem from the inherent difficultly of simulating quantum systems. Extensions of computer science using quantum mechanics led to the exploitation of the novel effects of quantum mechanics for computational purposes resulting in several proposals for quantum computers [4]. Quantum simulation is the idea of using quantum computational devices for more efficient simulation [5, 6]. Since the dynamics are simulated

*Corresponding author. Email: aspuru@chemistry.harvard.edu.

by a quantum system rather than calculated by a classical system, quantum simulation often offers exponential advantage over classical simulation for calculation of electronic energies [7], reaction rates [8, 9], correlation functions [10] and molecular properties [11]. Recently, a review of these techniques and other applications of quantum computing to chemistry has appeared [12].

The state of the art in experimental realizations of quantum simulation for chemistry is represented by calculations of the energy spectrum of molecular hydrogen first by Lanyon et al. [13] using an optical quantum computer. Very soon after, Du et al. [14] used NMR technology to demonstrate the adiabatic state preparation procedure suggested by Ref. [7] as well as reproduce the energy to higher accuracy.

The key limitation of both experimental algorithms was the representation of the simulated system's propagator. Both experiments, relied on the low dimensionality of the propagator for the minimal basis H_2 model considered. The unitary propagator for a two-level system can be decomposed using the real angles α, β, γ:

$$U = e^{i\alpha} R_y(\beta) R_z(\gamma) R_y(-\beta)$$

Due to this decomposition, longer propagation times corresponding to higher powers of unitary evolution operator, U^j, can be achieved by changing α to $j\alpha$ and γ to $j\gamma$, thereby avoiding the need of further decomposition of the unitary operator. Beyond the two dimensional case, this decomposition is not available.

The objective of this paper is to provide a general decomposition for electronic Hamiltonians and demonstrate this method with an explicit quantum circuit for a single Trotter time step of the minimal basis hydrogen molecule. This is an extension of the supplementary material from Lanyon et al. [13]. The construction of the general quantum circuit to simulate the propagator is performed in three steps:

(1) Write the Hamiltonian as a sum over products of Pauli spin operators acting on different qubits. This is described in Section 2 and made possible by the Jordan-Wigner transformation.
(2) Convert each of the operators defined in step (1) into unitary gates such that their sequential execution on a quantum copmuter can be made to recover an approximation to the full unitary propagator. This is detailed in Section 3.
(3) The phase estimation algorithm, as described in Section 4, is then used to approximate the eigenvalues of an input eigenstate using the propagator created in step (2) to perform spectral analysis. Section 5 discusses eigenstate preparation.

To demonstrate these steps, the construction is applied to the example of the hydrogen molecule in Section 6. The key components of the simulation procedure are depicted in Fig. 1. The next section provides a basic review of the fundamental concepts and notations of molecular quantum chemistry for the benefit of quantum information scientist and to establish the notation. A detailed account of electron structure methods can be found in the monographs [1, 2].

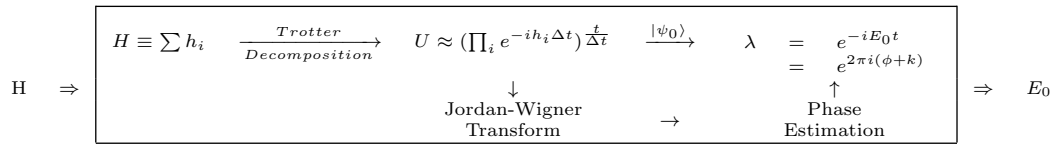

Figure 1. An algorithmic overview of the steps taken to simulate a chemical Hamiltonian on a quantum computer. The time independent Hamiltonian of a molecular system (to the left of the box) will be decomposed into a sum of Hermitian matrices, (h_i) and by means of a Trotter decomposition the unitary propagator U can be constructed. The Jordan-Wigner mapping is used to convert the propagator into a sequence of quantum gates. Phase estimation algorithms are used to evaluate the eigenvalue of a correctly prepared stationary state $|\psi_0\rangle$.

2. The Electronic Hamiltonian

The Born-Oppenheimer approximation assumes that the wave function of a molecule can be expressed as a product state of the nuclear and electronic wave functions due to the separation of time scales due to the difference in mass between electron and nuclei. This approximation allows for the solution of the time independent Schrödinger equation of the electronic wave function for a given nuclear geometry.

The molecular electronic Hamiltonian[1] in second quantized form is given by [1, 2]:

$$H = \sum_{p,q} h_{pq} a_p^\dagger a_q + \frac{1}{2} \sum_{p,q,r,s} h_{pqrs} a_p^\dagger a_q^\dagger a_r a_s, \tag{1}$$

where the sum is over the single particle basis set described below. The annihilation $\{a_j\}$ and creation operators $\{a_j^\dagger\}$ obey the Fermionic anti-commutation relations (see Table 1):

$$[a_p,\ a_q]_+ = 0, \qquad\qquad [a_p,\ a_q^\dagger]_+ = \delta_{pq}\mathbf{1}, \tag{2}$$

where the anti-commutator of operators A and B is defined as $[A, B]_+ \equiv AB + BA$. The annihilation (creation) operators correspond to a set of orbitals, $\{\chi_i\}$, where each orbital is a single-particle wave function composed of a spin and a spatial function, denoted σ_i and φ_i, respectively. As the Hamiltonian commutes with the electron spin operators, σ_i is restricted to be one of two orthogonal functions of a spin variable ω that we denote $\alpha(\omega)$ and $\beta(\omega)$. Similar Hamiltonians can be found in many physics problems involving Fermionic particles.

Although any basis can be used, the molecular orbitals are particularly convenient for state preparation reasons discussed below. The molecular orbitals, in turn, are formed as a linear combinations of atomic basis functions [15, 16]. The coefficients of this expansion are obtained by solving the set of Hartree-Fock equations which arise from the variational minimization of the energy using a single determinant. Due to its restriction to a single determinant, the Hartree-Fock solution is a mean field solution and the difference between the Hartree-Fock solution using an infinite basis of atomic orbitals and the exact (correlated) solution defines the electron correlation energy.

The matrix elements $\{h_{pq}\}$ and $\{h_{pqrs}\}$ in Eq. (1) denote the set of one- and two-electron integrals that must be evaluated using a known set of basis func-

[1]Throughout this paper, atomic units are used: $\hbar$ ($1.054 \cdot 10^{-34}$ J s), the mass of the electron ($9.109 \cdot 10^{-31}$ kg), the elementary charge ($1.602 \cdot 10^{-19}$ C), and the electrostatic force constant ($1/4\pi\epsilon_0 = 8.988 \cdot 10^9$ N m^2 C^{-2}) are set to unity.

Table 1. An overview of second quantization for Fermionic particles. For quantum chemistry, the annihilation and creation operators correspond to removing (adding) an electron into a particular orbital, $\{\chi_k\}$. The anti-symmetry is enforced by the canonical commutation relations, and the N-electron wave function is expanded over the configuration state functions of the Fock space.

Second quantization		
Creation operator	$a_i^\dagger \vert j_1,\ldots,0_i,\ldots,j_n\rangle = \Gamma_i^{\mathbf{j}} \vert j_1,...,1_i,...,j_n\rangle$ $a_i^\dagger \vert j_1,\ldots,1_i,\ldots,j_n\rangle = 0$	with $\Gamma_i^{\mathbf{j}} = \prod_{n=1}^{i-1}(-1)^{j_n}$
Annihilation operator	$a_i \vert j_1,\ldots,1_i,\ldots,j_n\rangle = \Gamma_i^{\mathbf{j}} \vert j_1,...,0_i,...,j_n\rangle$ $a_i \vert j_1,\ldots,0_i,\ldots,j_n\rangle = 0$	
Canonical commutation relations	$\{a_i^\dagger, a_j\} = \delta_{ij}\mathbf{1}$ $\{a_i, a_j\} = 0$	

Fock space		
Basis vectors, configuration state functions	$\vert\mathbf{j}\rangle = \vert j_1, j_2, ..., j_N\rangle$ $= \prod_{p=1}^N \left(a_p^\dagger\right)^{j_p} \vert vac\rangle$	where $j_i = 0, 1$
Inner product	$\langle\mathbf{j}\vert\mathbf{k}\rangle = \prod_{p=1}^N \delta_{j_p,k_p}$	
Vacuum state	$\langle vac\vert vac\rangle = 0$ $a_i \vert vac\rangle = 0$	
Operator, $\hat{A}$	$\hat{A}_{ij} a_i^\dagger a_j$	where $\hat{A}_{ij}$ is evaluated in the mode space corresponding to $\{a_k\}$

tions (the basis set) during the Hartree-Fock procedure. Ideally, the number of basis functions used would be infinite, but in practice only a finite number of basis functions are used. By selecting Gaussian functions single-particle basis functions, these integrals are efficiently computable. Next, to further establish notation, we develop the explicit form of the integrals h_{pq} and h_{pqrs}.

We denote the set of single-particle spatial functions which constitute the molecular orbitals $\{\varphi_k(x)\}_{k=1}^M$. Finally, define the set of spin orbitals as $\{\chi_p(\mathbf{x})\}_{p=1}^{2M}$ with $\chi_p = \varphi_i\sigma_i$ and $\mathbf{x} = (x, \omega)$ where σ_i is a spin function. In the following equations for the one- and two-electron integrals, we identify $\chi_p = \varphi_i\sigma_i, \chi_q = \varphi_j\sigma_j, \chi_r = \varphi_k\sigma_k$, and $\chi_s = \varphi_l\sigma_l$. The one-electron integrals involving the electron's kinetic energy and the electron-nuclear attraction terms:

$$\begin{aligned} h_{pq} &\equiv \int \mathrm{d}\mathbf{x}\, \chi_p^*(\mathbf{x}) \left(-\frac{1}{2}\nabla^2 - \sum_\alpha \frac{Z_\alpha}{r_{\alpha,\mathbf{x}}}\right) \chi_q(\mathbf{x}) \\ &= \langle\varphi_i\vert H^{(1)}\vert\varphi_j\rangle\, \delta_{\sigma_i\sigma_j}. \end{aligned} \tag{3}$$

and the two-electron integrals involving the electron-electron interaction, $1/r_{12}$:

$$\begin{aligned} h_{pqrs} &\equiv \int \mathrm{d}\mathbf{x}_1 \mathrm{d}\mathbf{x}_2 \frac{\chi_p^*(\mathbf{x}_1)\chi_q^*(\mathbf{x}_2)\chi_r(\mathbf{x}_2)\chi_s(\mathbf{x}_1)}{r_{1,2}} \\ &= \langle\varphi_i\vert\langle\varphi_j\vert H^{(2)}\vert\varphi_k\rangle\vert\varphi_l\rangle \delta_{\sigma_i\sigma_j}\delta_{\sigma_k\sigma_l}. \end{aligned} \tag{4}$$

In Eq. (3), ∇^2 is the Laplacian with respect to the electron spatial coordinates. The positive valued scalars $r_{\alpha,\mathbf{x}}$ and $r_{1,2}$ are the Euclidean distance between the α^{th} nucleus and the electron and the Euclidean distance between the two electrons.

2.1. *Representing the molecular Hamiltonian in terms of quantum bits*

Just as classical computation is based on the notion of a bit, the basic unit of quantum information is the quantum bit (qubit). In principle, any two-level quantum mechanical system can be considered a qubit. Practical requirements for qubits and their manipulation was originally outlined by DiVincenzo [17] and experimental progress towards satisfying the DiVincenzo criteria was recently reviewed [4]. Since two-level systems can be described as spin-half particles, the relevant (Pauli) spin matrices are:

$$\sigma^x = \begin{bmatrix} 0 & 1 \\ 1 & 0 \end{bmatrix} \qquad \sigma^y = \begin{bmatrix} 0 & -i \\ i & 0 \end{bmatrix} \qquad \sigma^z = \begin{bmatrix} 1 & 0 \\ 0 & -1 \end{bmatrix}.$$

Together with the identify matrix, the Pauli matrices form an operator basis for two-level systems. The basis of σ^z is called the computational basis with $|0\rangle$ ($|1\rangle$) labeling the upper (lower) eigenstate. There are several computationally equivalent models of describing quantum computation but here we focus on the circuit model of quantum computation. A more comprehensive introduction of quantum computation can be found in Ref. [18].

The quantum circuit model uses a set of elementary gates to reproduce the action of arbitrary unitary transforms. A universal gate set requires single qubit gates and any two-qubit entangling gate. The two-qubit CNOT gate leaves one qubit space invariant and acts with σ^x on the second qubit when the first qubit is in the state $|1\rangle$. The gate is given as $\mathsf{CNOT} = |1\rangle\langle 1| \otimes \sigma^x + |0\rangle\langle 0| \otimes \mathbf{1}$. The set, R_x, R_y, and R_z gates can generate any single qubit gate were R_n is defined as $\exp[-i\sigma^n\theta/2]$ for real θ.

For experimental addressability, the qubits must, in general, be distinguishable. However, the electrons of the molecular system are indistinguishable. The Jordan-Wigner transform is used to circumvent this issue by expressing Fermionic operators in terms of the Pauli spin operators $\{\sigma^x, \sigma^y, \sigma^z, \mathbf{1}\}$ that correspond to the algebra of distinguishable spin 1/2 particles [10, 19]. The Jordan-Wigner transform is given by:

$$a_j \Leftrightarrow \mathbf{1}^{\otimes j-1} \otimes \sigma^+ \otimes \sigma^{z \otimes N-j-1} \tag{5a}$$

$$a_j^\dagger \Leftrightarrow \mathbf{1}^{\otimes j-1} \otimes \sigma^- \otimes \sigma^{z \otimes N-j-1} \tag{5b}$$

where $\sigma^+ \equiv \frac{\sigma^x + i\sigma^y}{2} = |0\rangle\langle 1|$ and $\sigma^- \equiv \frac{\sigma^x - i\sigma^y}{2} = |1\rangle\langle 0|$. The qubit state $|0 \ldots 0\rangle$ corresponds to the vacuum state and the string of σ^z operators, preserve the commutation relations in Eq. (2) since σ^z and $\sigma^\pm$ anti-commute. The spin variable representation of relevant operators after the Jordan-Wigner transformation is given in Table A2 found in the appendix.

3. Efficient approximations of the unitary propagator by a Trotter decomposition

A key element of the quantum computer simulation scheme that aids in achieving an exponential speed up over classical computation involves the use the Trotter-Suzuki formula, given below, where the quantum circuit for the unitary propagator is given by a composition of smaller circuits that correspond to the exponential of each of N^4 two-electron terms and each of the N^2 one-electron terms of Eq. (1). The advantage of using such a decomposition for a

quantum computer is that one does not need to access nor directly optimize the parameters of the full N-body wave function. The number of parameters grows rapidly with system size and description hindering methods like full configuration interaction (FCI), but in a quantum computer measurement collapses the wave function to the desired state. To perform quantum measurement as described in Section 4, it suffices to execute the circuit corresponding to the Trotter-Suzuki for a sufficiently-small time step. Next, we describe the quantum circuits for the exponential of the products of Pauli operators necessary for simulating Jordan-Wigner transformed operators. The Trotter-Suzuki approach is explained below.

3.1. *Quantum circuit primitives*

Each term of Eq. (1) can be exponentiated using the universal gate set described in Subsection 2.1 after performing the Jordan-Wigner transformation to Pauli spin matrices. We will outline the procedure for generating quantum circuits for chemical systems and summarise the results in Fig. A1. The construction of quantum circuits for general Fermionic Hamiltonians is further discussed in Ref. [10, 20, 21].

To understand the exponential map of the product of Pauli spin matrices, first consider the exponential map of two σ^z operators. To create the unitary gate $\exp[-i\frac{\theta}{2}(\sigma^z \otimes \sigma^z)]$, the CNOT gate can be used to first entangle two qubits, then the R_z gate is applied, followed by a second CNOT gate that disentangles the qubit pair [18].

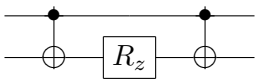

This construction can be generalized to more qubits by using additional CNOT gates. For example, the circuit for the three-body operator involving three qubits, $\exp[-i\frac{\theta}{2}(\sigma^z \otimes \sigma^z \otimes \sigma^z)]$, is simulated by the following quantum circuit:

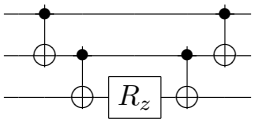

As seen from the three-qubit example above, this construction can be readily extended for n-fold products of σ^z operators.

3.1.1. Construction of different Pauli matrix products

If one requires a different product of Pauli matrices besides the product of σ^z as described above, a change of basis can be accomplished using the appropriate unitary transformation: Hadamard transforms between σ^x basis and σ^z basis, and $\mathsf{Y} = R_x(-\pi/2) = \exp(i\sigma^x\pi/4)$ transforms from σ^z basis to σ^y basis and $\mathsf{Y}^\dagger$ from σ^y to σ^z. In matrix form,

$$\mathsf{H} = \frac{1}{\sqrt{2}}\begin{bmatrix} 1 & 1 \\ 1 & -1 \end{bmatrix} \qquad \mathsf{Y} = \frac{1}{\sqrt{2}}\begin{bmatrix} 1 & i \\ i & 1 \end{bmatrix}.$$

Circuits of this form form the basis for the construction of the molecular unitary propagator as illustrated in Fig. A1 where the circuit representations are given.

3.2. *Trotter decomposition*

Using the second-quantized representation allows for a straightforward decomposition of the exponential map of each term of the Hamiltonian. However, the terms of this decomposition do not always commute. The goal of the Trotter decomposition is to approximate the time evolution operator of a set of non-commuting operators. The operators are exponentiated individually for small time steps and the procedure is repeated such that their product provides a reasonable approximation to the exponentiation of the sum. Using this approximation, the construction of the time propagator can be efficiently carried out on a quantum computer provided that the Hamiltonian can be decomposed into a sum of local Hamiltonians [6]. The first-order Trotter decomposition is given by:

$$e^{-iHt} = \left(e^{-ih_1\Delta t}e^{-ih_2\Delta t}\cdots e^{-ih_N\Delta t}\right)^{\frac{t}{\Delta t}} + O(t\Delta t), \tag{6}$$

where $t/\Delta t$ is the Trotter number [22]. As the Trotter number tends to infinity, or equivalently $\Delta t \to 0$, the error in the approximation vanishes. If $t/\Delta t$ is not an integer, the remainder is simulated as another Trotter time slice. There exist higher order approximates (Suzuki-Trotter formulas) which reduce the error of approximation even further. For instance, the second order approximations is given by:

$$e^{-iHt} \approx \left(\left(e^{-ih_1\frac{\Delta t}{2}}\cdots e^{-ih_{N-1}\frac{\Delta t}{2}}\right)e^{-ih_N\Delta t}\left(e^{-ih_{N-1}\frac{\Delta t}{2}}\cdots e^{-ih_1\frac{\Delta t}{2}}\right)\right)^{\frac{t}{\Delta t}} + O(t(\Delta t)^2). \tag{7}$$

Higher order approximations take increasingly more complicated forms [22] and were first studied in the context of black box quantum simulation of sparse Hamiltonians by Berry *et al.* [23]. They considered Hamiltonians composed of m efficiently implementable terms and showed that the number of exponentials cannot scale better than linear in the time desired and the maximum frequency of the full Hamiltonian. The proof shows that if sublinear simulation of arbitrary Hamiltonians were possible, bounds for the power of quantum computation proven in Ref. [24] could be violated leading to a contradiction.

4. The phase estimation algorithm

In this section, we describe how to obtain molecular energies given the time evolution of the molecular Hamiltonian described above. The time propagator of the Hamiltonian, along with a stationary state, can be used to convert eigenvalues into relative phases. The relative phase can then be obtained using the quantum phase estimation algorithm (PEA). To determine an eigenvalue associated with an eigenstate, consider the phase an eigenstate of the Hamiltonian H evolving dependent on a register qubit:

$$|0\rangle|\psi_n\rangle + e^{-iHt}|1\rangle|\psi_n\rangle = |0\rangle|\psi_n\rangle + e^{-iE_nt}|1\rangle|\psi_n\rangle. \tag{8}$$

By letting $E_n = 2\pi(\phi - K)/t$ where K is an integer and $0 \leq \phi < 1$, the unknown eigenvalue becomes encoded in the relative phase of the register qubit quantum state as $|0\rangle + e^{-2\pi i(\phi-K)}|1\rangle$ [7, 25, 26]. The binary expansion

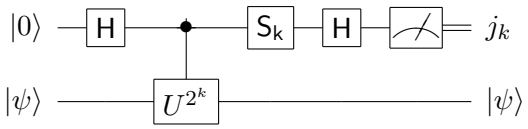

Figure 2. Iterative phase estimation circuit for obtaining the k^{th} qubit. The phase is represented using a binary decimal expansion $\phi = 0.j_0j_1j_2j_3\cdots j_n$. To gain precision in the algorithm, one adjusts the parameterized gate $\mathsf{S_k}$ according to the values of all previous obtained bits. This U is a representation of the propagator of the system being simulated. Acting on the eigenstate with this operator advances the phase of the state.

of ϕ:

$$\phi = 0.j_0j_1j_2j_3\cdots = \left(\frac{j_0}{2}\right) + \left(\frac{j_1}{4}\right) + \left(\frac{j_2}{8}\right) + \left(\frac{j_3}{16}\right) + \ldots \tag{9}$$

can then be recovered from measurements performed on the register qubits.

The PEA can be accomplished in several different ways depending on the technology available and in the recent experimental implementations, the iterative phase estimation algorithm [25, 27–29] was used. We present it here for completeness.

The iterative method relies on the use of the gate $\mathsf{S_k}$ depicted in Fig. 2. Data is read from the least significant digit first, allowing the counter-rotation $\mathsf{S_k}$ to be a function of the $L-k-1$ digits that were previously obtained where L is the least significant digit of the binary expansion. The form of the $\mathsf{S_k}$ gate is given by:

$$\mathsf{S_k} = \begin{bmatrix} 1 & 0 \\ 0 & \Phi_k \end{bmatrix}, \quad \text{with} \quad \Phi_k = \exp\left[2\pi i \sum_{l=2}^{L-k+1} \frac{j_{k+l-1}}{2^l}\right].$$

This gate removes the $L-k-1$ least significant digits so the state of quantum computer becomes, $(|0\rangle + \exp[-i\pi j_k]|1\rangle)|\psi_n\rangle$ where j_k is zero or one. Finally, effecting the Hadamard transformation described in Section 3.1.1 leads to $|j_k\rangle|\psi_n\rangle$ and measurement of the register in the $\{|0\rangle, |1\rangle\}$ basis yields the value of j_k. When the binary expansion of ϕ is length L, the measurements are deterministic, otherwise the remainder can cause errors as discussed in Refs. [18, 28].

The evolution of the eigenstate must be dependent on the register qubit requiring that the construction of the unitary evolution operator described in Section 3.1 be modified. The constructions listed in Fig. A1 only need to be slightly modified; since the underlying constructions rely on R_z gates, changing these rotations into controlled R_z rotations ($|1\rangle\langle 1|\otimes R_z + |0\rangle\langle 0|\otimes \mathbf{1}$) is sufficient to make the entire unitary dependent on the readout qubit.

Once an estimated phase is obtained, it must be inverted to obtain the energy. Given bounds for the energy eigenvalue, $[E_{min}, E_{max})$, the time of evolution is selected as $E_{max} - E_{min} = 2\pi/t \equiv \omega$ and an energy shift of E_s is used to make $(E_s - E_{min})/\omega$ an integer and then $K = (E_s - E_{min})/\omega$. The energy shift E_s when obtaining the k-th bit of ϕ is effected by a gate on the register qubit which applies a phase of $\exp(i2^kE_st)$ to the qubit if it is in state $|1\rangle$ and does nothing otherwise. Using these parameters the measured value of ϕ corresponds to the value of the energy, $E_\phi = \omega(\phi - K) + E_s$.

As noted in Ref. [30], in phase estimation algorithm the number of uses of

$U(t)$ scales exponentially with the number of bits desired from ϕ. This is a consequence of the Fourier uncertainty principal; the more information required in the frequency domain the longer the propagation time. When the unitary is decomposed into gates, this means an exponential increase in the gates is required for an exponential increase in the precision of the measurement.

To obtain the correct values of j_n from Eq. (9), the PEA relies on the assumption that the input vector to the algorithm is close to an eigenvector of the controlled unitary operator being used. Since each qubits represents the occupancy of molecular orbitals in the N-electron wave function, the HF guess for the ground state $|\psi_0^{HF}\rangle$ requires no superposition of states and is thus straightforward to prepare. For $|\langle\psi_0^{HF}|\psi_0^{FCI}\rangle| = 1 - \epsilon$, where ϵ is small, the phase estimation algorithm can be applied to retrieve an estimate of the ground state energy. Simultaneously, the state of the system will collapse to $|\psi_0^{FCI}\rangle$ when measured in the H^{FCI} basis (via PEA) with high probability [25, 26]. If the Hartree-Fock guess is insufficient, more sophisticated state preparation procedures exist and these were reviewed in Ref. [12]. The adiabatic scheme for state preparation [7] is analyzed in the following section.

5. Adiabatic state preparation

This section explains the method of preparing an input state to the simulation algorithm using adiabatic quantum computation [7, 31, 32]. First, consider the Hartree-Fock wave function as an approximation to the FCI wave function. This is the output of an classical algorithm returning, in polynomial time, a computational basis state where the qubits which correspond to occupied molecular orbitals are in the state $|1\rangle$ with the remaining qubits in state $|0\rangle$. To increase overlap of the wave function, after the system is prepared in state $|\psi_0^{HF}\rangle$, the Hamiltonian H_{FCI} is slowly applied and the actual ground state is recovered by adiabatic evolution. Consider a smooth one-parameter family of adiabatic path Hamiltonians,

$$H(s) = (1 - s)H_{HF} + sH_{FCI}, \tag{10}$$

for monotonic $s \in [0, 1]$. This was the adiabatic path originally proposed by us in Ref. [7]. Other paths may be used as in Ref. [33] but in this study we restrict our attention to evolution of the form in Eq. (10).

Let the instantaneous energies of $H(s)$ be given by the sequence,

$$E_0(s) < E_1(s) \leq \cdots \leq E_{N-1}(s), \tag{11}$$

then the adiabatic state preparation procedure is efficient whenever the total run time, T, satisfies the following:

$$T \gg \min_{0 \leq s \leq 1} \left(E_1(s) - E_0(s)\right)^{-2}, \tag{12}$$

according to known results relating the adiabatic theorem to complexity theory [31]. After adiabatic evolution, the state of the system is $|\psi_0^{FCI}\rangle$, which is the ground state of the molecular Hamiltonian H_0^{FCI}. Modified versions of this procedure exist using decoherence to achieve faster evolution and are discussed in Refs. [34, 35].

Assume that the adiabatic evolution induced transitions into higher energy

Table 2. The one-electron and two-electron integrals defined in Eqs. (3) and (4) are evaluated using the molecular spatial orbitals obtained from a restricted Hartree-Fock calculation at an internuclear distance of 1.401000 atomic units ($7.414{\cdot}10^{-11}$ m) [42].

Spatial integral	Value (a.u.)
$h_{\varphi_1\varphi_1}$	-1.252477
$h_{\varphi_2\varphi_2}$	-0.475934
$h_{\varphi_1\varphi_2}$	0
$h(\varphi_1\varphi_1\varphi_1\varphi_1)$	0.674493
$h(\varphi_2\varphi_2\varphi_2\varphi_2)$	0.697397
$h(\varphi_2\varphi_1\varphi_1\varphi_2)$	0.663472
$h(\varphi_1\varphi_2\varphi_1\varphi_2)$	0.181287
$h(\varphi_1\varphi_1\varphi_2\varphi_2)$	0.181287
$h(\varphi_2\varphi_2\varphi_1\varphi_1)$	0.181287

states and so the un-normalized state of the system is $|\psi_0^{FCI}\rangle + \lambda|k\rangle$, where $|k\rangle \in \mathcal{H} = 1 - |\psi_0^{FCI}\rangle\langle\psi_0^{FCI}|$. While the error in the wave function is linear in $\lambda < 1$, the overestimate of the energy in the expectation value $\langle H_0^{FCI}\rangle$ is only quadratic.

It is unclear how this method will scale. It is possible to prepare a desired ground state efficiently provided that the gap between the ground and excited states is sufficiently large [31]. This depends on the adiabatic path taken. Finding the ground state energy of a random Hamiltonian, even for simple models, is known to be complete for the quantum analogue of the class NP [36, 37].

There are other ways to perform state preparation, for example, by going beyond Hartree-Fock theory [38, 39]. A broader discussion of state preparation for quantum simulation can be found in Refs. [12, 40]. Recently, in Ref. [41], the effects of initial states for the phase estimated quantum simulation CH_2 molecules was studied for a variety of geometries and eigenstates using initial guesses obtained via multi-configuration approaches.

6. Simulating the hydrogen molecule

To illustrate the algorithmic details of a scalable simulation of quantum systems, the hydrogen molecule in a minimal basis is used as an instructive example. The minimal basis is the minimum number of spatial-functions needed to describe the system and in the case of H_2, one spatial-function is needed per atom denoted φ_{H1} and φ_{H2}. In this simple case, the Hartree-Fock procedure is not necessary as the molecular spatial-orbitals are determined by symmetry and are given by $\varphi_u = \varphi_{H1} + \varphi_{H2}$ and $\varphi_g = \varphi_{H1} - \varphi_{H2}$. These two spatial functions correspond to four orbitals that will be identified as:

$$|\chi_1\rangle = |\varphi_g\rangle|\alpha\rangle, \quad |\chi_2\rangle = |\varphi_g\rangle|\beta\rangle, \quad |\chi_3\rangle = |\varphi_u\rangle|\alpha\rangle, \quad |\chi_4\rangle = |\varphi_u\rangle|\beta\rangle. \quad (13)$$

The form of the spatial function is determined by the basis set used. The STO-3G basis is a common minimal basis that approximates a single electron spatial Slater type orbitals (STO), with a contraction of three real Gaussian functions [1]. Using this orbital basis, the spatial integrals of the Hamiltonian were evaluated in Table 2 for H_2 at bond distance 1.401000 atomic units ($7.414{\cdot}10^{-11}$ m).

Considering H from Eq. (1) as $H^{(1)} + H^{(2)}$ we have,,

$$H^{(1)} = h_{11}a_1^\dagger a_1 + h_{22}a_2^\dagger a_2 + h_{33}a_3^\dagger a_3 + h_{44}a_4^\dagger a_4 \tag{14}$$

The following circuit applies the single-electron propagator for a time t:

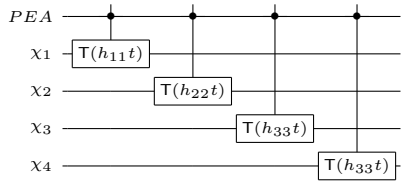

The gate T is defined as:

$$\boxed{\mathsf{T}(\theta)} = \begin{bmatrix} 1 & \\ & e^{-i\theta} \end{bmatrix}. \tag{15}$$

The two electron Hamiltonian can also be expanded. As electrons are indistinguishable,

$$h_{pqrs} = \int \mathrm{d}\mathbf{x}_1\mathrm{d}\mathbf{x}_2 \frac{\chi_p(\mathbf{x}_1)\chi_q(\mathbf{x}_2)\chi_r(\mathbf{x}_2)\chi_s(\mathbf{x}_1)}{r_{12}} = \int \mathrm{d}\mathbf{x}_2\mathrm{d}\mathbf{x}_1 \frac{\chi_p(\mathbf{x}_2)\chi_q(\mathbf{x}_1)\chi_r(\mathbf{x}_1)\chi_s(\mathbf{x}_2)}{r_{12}} = h_{qpsr},$$

and $a_p^\dagger a_q^\dagger a_r a_s = a_q^\dagger a_p^\dagger a_s a_r$, the two electron Hamiltonian can be simplified as:

$$\begin{aligned} H^{(2)} = {} & h_{1221}a_1^\dagger a_2^\dagger a_2 a_1 + h_{3443}a_3^\dagger a_4^\dagger a_4 a_3 + h_{1441}a_1^\dagger a_4^\dagger a_4 a_1 + h_{2332}a_2^\dagger a_3^\dagger a_3 a_2 \\ & + (h_{1331} - h_{1313})\, a_1^\dagger a_3^\dagger a_3 a_1 + (h_{2442} - h_{2424})\, a_2^\dagger a_4^\dagger a_4 a_2 \\ & + \Re(h_{1423})(a_1^\dagger a_4^\dagger a_2 a_3 + a_3^\dagger a_2^\dagger a_4 a_1) + \Re(h_{1243})(a_1^\dagger a_2^\dagger a_4 a_3 + a_3^\dagger a_4^\dagger a_2 a_1) \\ & + \Im(h_{1423})(a_1^\dagger a_4^\dagger a_2 a_3 - a_3^\dagger a_2^\dagger a_4 a_1) + \Im(h_{1243})(a_1^\dagger a_2^\dagger a_4 a_3 - a_3^\dagger a_4^\dagger a_2 a_1) \end{aligned} \tag{16}$$

The first six terms,

$$\begin{aligned} & h_{1221}a_1^\dagger a_2^\dagger a_2 a_1 + h_{3443}a_3^\dagger a_4^\dagger a_4 a_3 + h_{1441}a_1^\dagger a_4^\dagger a_4 a_1 \\ & + h_{2332}a_2^\dagger a_3^\dagger a_3 a_2 + (h_{1331} - h_{1313})\, a_1^\dagger a_3^\dagger a_3 a_1 + (h_{2442} - h_{2424})\, a_2^\dagger a_4^\dagger a_4 a_2 \end{aligned}$$

can be simulated using the system Hamiltonian that employs only commuting two-local terms described in Section 3. Notice after the Jordan-Wigner transform of the relevant operator we have:

$$\begin{aligned} \sum_{p<q}(h_{pqqp} - h_{pqpq}\delta_{\sigma_p\sigma_q})a_p^\dagger a_q^\dagger a_q a_p = {} & \left(\frac{1}{4}\sum_{p<q}(h_{pqqp} - h_{pqpq}\delta_{\sigma_p\sigma_q})\right)\mathbf{1} \\ & -\frac{1}{4}\sum_q\left(\sum_{p\neq q}(h_{pqqp} - h_{pqpq}\delta_{\sigma_p\sigma_q})\right)\sigma_q^z \\ & +\sum_{p<q}\frac{(h_{pqqp} - h_{pqpq}\delta_{\sigma_p\sigma_q})}{4}\sigma_p^z\sigma_q^z. \end{aligned} \tag{17}$$

The factor of $1/2$ is accounted for because the indistinguishably of the electrons reduces the summation in Eq. (1).

Following Eq. (17), let $\Theta \equiv (1/4)\sum_{p<q}(h_{pqqp} - h_{pqpq}\delta_{\sigma_p\sigma_q})$ and $\theta_p \equiv \sum_{q:p\neq q}(h_{pqqp} - h_{pqpq}\delta_{\sigma_p\sigma_q})$. Then following circuit illustrates the one and two-local interactions required to implement Eq. (17):

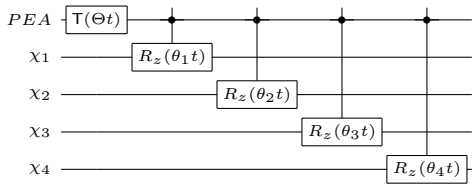

Defining $\eta_{pq} \equiv \frac{1}{4}(h_{pqqp} - h_{pqpq}\delta_{\sigma_p\sigma_q})$, the three local interactions can be depicted as:

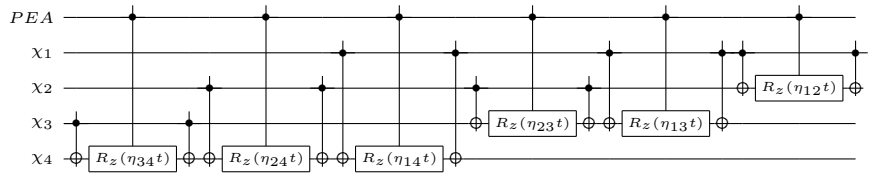

Each term commutes thus can be realized in any order.

The remaining terms are strictly real leaving:

$$h_{1423}(a_1^\dagger a_4^\dagger a_2 a_3 + a_3^\dagger a_2^\dagger a_4 a_1) + (h_{1243})(a_1^\dagger a_2^\dagger a_4 a_3 + a_3^\dagger a_4^\dagger a_2 a_1).$$

Since the orbitals are real, the integrals $h_{1243} = h_{1423}$ are equivalent. Therefore, we are left with the task of simulating $2h_{1423}(a_1^\dagger a_4^\dagger a_2 a_3 + a_3^\dagger a_2^\dagger a_4 a_1)$.

Consider the general term $a_p^\dagger a_q^\dagger a_r a_s + a_s^\dagger a_r^\dagger a_q a_p$. Due to the anti-commutation rules, all sets of operators corresponding to a set of four distinct spin-orbitals, (p, q, r, s), are simulated using the same circuit. This is due to the fact that the Jordan-Wigner of each operator generates same set of operators (namely, the eight combinations involving an even number of σ^x and σ^y operators). However, depending on if σ^+ or σ^- is used each term of spin operators will have a different sign. If we define:

$$h^{(1)} = (h_{pqrs}\delta_{\sigma_p\sigma_s}\delta_{\sigma_q\sigma_r} - h_{qprs}\delta_{\sigma_p\sigma_r}\delta_{\sigma_q\sigma_s}) \tag{18}$$

$$h^{(2)} = (h_{psqr}\delta_{\sigma_p\sigma_r}\delta_{\sigma_q\sigma_s} - h_{spqr}\delta_{\sigma_p\sigma_q}\delta_{\sigma_r\sigma_s}) \tag{19}$$

$$h^{(3)} = (h_{prsq}\delta_{\sigma_p\sigma_q}\delta_{\sigma_r\sigma_s} - h_{prqs}\delta_{\sigma_p\sigma_s}\delta_{\sigma_q\sigma_r}) \tag{20}$$

then

$$\frac{1}{2}\sum h_{pqrs}a_p^\dagger a_q^\dagger a_r a_s + a_s^\dagger a_r^\dagger a_q a_p = \frac{1}{8}\left(\bigotimes_{k=p+1}^{q-1}\bigotimes_{k=r+1}^{s-1}\sigma_k^z\right) \tag{21}$$

$$\begin{pmatrix} (\sigma_p^x\sigma_q^x\sigma_r^x\sigma_s^x + \sigma_p^y\sigma_q^y\sigma_r^y\sigma_s^y)(-h^{(1)} - h^{(2)} + h^{(3)}) \\ +(\sigma_p^x\sigma_q^x\sigma_r^y\sigma_s^y + \sigma_p^y\sigma_q^y\sigma_r^x\sigma_s^x)(+h^{(1)} - h^{(2)} + h^{(3)}) \\ +(\sigma_p^y\sigma_q^x\sigma_r^y\sigma_s^x + \sigma_p^x\sigma_q^y\sigma_r^x\sigma_s^y)(-h^{(1)} - h^{(2)} - h^{(3)}) \\ +(\sigma_p^y\sigma_q^x\sigma_r^x\sigma_s^y + \sigma_p^x\sigma_q^y\sigma_r^y\sigma_s^x)(-h^{(1)} + h^{(2)} + h^{(3)}) \end{pmatrix}.$$

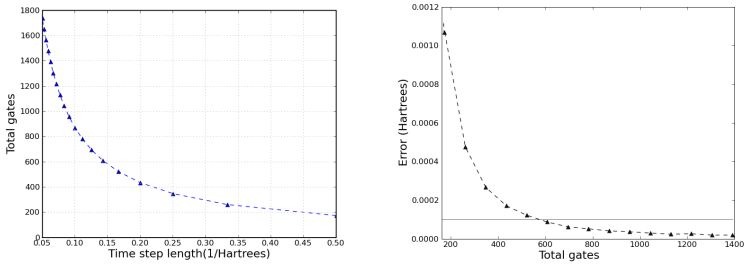

(a) Plot of gates to simulate the H_2 versus time step used in the first order Trotter approximation. *(b)* Plot of relative error of approximation as a function of gates used.

Figure 3. The unitary propagator corresponding to this Hamiltonian is approximated using a first order Trotter decomposition and these graphs provide analysis of the Trotter error and the number of gates used at each Trotter number, T_n. The unitary propagator is simulated by applying each small term of the second quantized Hamiltonian for small time steps dt and repeating the process $T_n = t/dt$ times. As dt decreases the error in the approximation decreases at the expense of more gates. Zero error represents the eigenvalue of the Hamiltonian of H_2 in the minimal basis at a separation of 1.4 atomic units. The horizontal line of *(b)* represents the threshold for energy error of 10^{-4} atomic units.

Applying this to the hydrogen molecule, observe that $h^{(1)} = -h^{(2)}$ and $h^{(3)} = 0$ indicating that only the terms $\{\sigma^x\sigma^x\sigma^y\sigma^y, \sigma^y\sigma^y\sigma^x\sigma^x, \sigma^y\sigma^x\sigma^x\sigma^y, \sigma^x\sigma^y\sigma^y\sigma^x\}$ must be considered. The resulting quantum circuit is illustrated in Table A3 found in the appendix.

To assess the Trotter error, we simulated this circuit using a classical computer using the first-order Trotter decomposition. The pseudo-code for the H_2 simulation is given in Appendix A and the results are summarized in Fig. 3. Although the gates increase with the Trotter number, reducing the Trotter error of the dynamics is only practical if the measurement is precise enough to detect such errors. Thus, in practice, there is a balance between the Trotter number selected and the number of bits to be obtained by the measurement procedure.

7. Conclusions

In this paper, we mapped the full configuration interaction (FCI) method from quantum chemistry into a quantum algorithm. We reviewed the electronic structure problem, techniques of creating the simulated propagator, and explicitly illustrated this construction for H_2 for a single timestep of a first-order Trotter expansion.

Applicability of quantum simulation comes down to the ability to propagate the simulated system with a specified error tolerance. Since phase estimation is essentially a Fourier transform of the frequency of phase oscillations (which are proportional to the eigenenergy) to obtain more precise determination of the frequency, a longer propagation time is necessary. This longer time requires more manipulations of the computational system.

This paper does not consider the effect of errors, however it is an important consideration that needs to be taken into account. Quantum error correction methods have been developed to counteract the unwanted effect of quantum noise, however fault tolerant constructions require redundant qubits and only allow a discrete set of gates to be used [18, 43]. This is not a serious cause for concern as the conversion from a continuous set of gates to a discrete set

of gates only requires a poly-logarithmic overhead [44]. Last year, Clark et al. [45] estimated the resources required to compute the ground state of a one dimensional transverse Ising model and found, using experimental parameters from a proposed ion trap quantum computing implementation, that the fault tolerant constructions would be too costly for straight-forward applications to simulation. This suggests that quantum simulation without quantum error correction is more feasible for the near future.

In the coming future, small scale experiments such as the simulation of the circuits we have presented for H_2 on a quantum computer will likely be possible. Experimental realizations of quantum chemistry on quantum devices have only recently been achieved [13, 14]. We hope that the present paper will continue the interest by giving an example of a scalable construction of the unitary propagator for the H_2 molecule in an explicit form, which poses the next logical challenge for experimental realization.

Acknowledgements

We thank H. Wang, A. Dutoi, P. Love, and M. Mohseni. This work received funding from the Faculty of Arts and Sciences at Harvard University, Engineering and Physical Sciences Research Council grant EP/G003017/1 (JDB), Defense Advance Research Projects Agency under the Young Faculty Award (N66001-09-1-2101) (AA-G), the Camille and Henry Dreyfus Foundation (AA-G), the Sloan Foundation (AA-G) and the Army Research Office under contract W911-NF-07-0304 (JDW, AA-G).

Appendix A. Pseudo-code for hydrogen molecule simulation

Here the decomposition of the propagator of H_2 Hamiltonian is given using standard quantum gates. The entire unitary operator is controlled via the 'Register' qubit. This qubit (or qubits) would be measured using any of a variety of phase estimation techniques. Additionally, the non-commuting terms of the Hamiltonian introduce error which can be reduced using Trotter time slicing or by using higher order Trotter-Suzuki decompositions. The time slicing idea is to alternatively apply each of the non-commenting unitary operators each for a fraction of the total time. As the length of the time slices goes to zero the error of the approximation will as well. The single electron operators and the number-number operators commute amongst themselves. However, the two-body and one-body excitation-excitation operators do not commute with the other operators but each excitation-excitation operator (XXXX, XXYY, etc.) commute. Qubits are named: Register, Q1, Q2, Q3, Q4. The integrals are h_{ij} and h_{ijkl} are given in Table 2. Additionally, we define $n_{ij} = (h_{ijji} - h_{jiji})/4$. Note only h_{1313} and h_{2424} are the only non-zero terms due to spin orthogonality. Following the main text, Let $\Theta \equiv (1/4)\sum_{p<q}(h_{pqqp} - h_{pqpq}\delta_{\sigma_p\sigma_q})$ and $\theta_p \equiv \sum_{q:p\neq q}(h_{pqqp} - h_{pqpq}\delta_{\sigma_p\sigma_q})$.

Gate	Target qubit	Control qubit	Parameter
Hadamard	Register		
Single Electron Operators			
cPhase	Q1	Register	$h_{11}t$
cPhase	Q2	Register	$h_{22}t$
cPhase	Q3	Register	$h_{33}t$
cPhase	Q4	Register	$h_{44}t$
Two Electron Operators: number-number operator			
Phase	Register		Θt
cR_z	Q1	Register	$-\theta_1 t$
cR_z	Q2	Register	$-\theta_2 t$
cR_z	Q3	Register	$-\theta_3 t$
cR_z	Q4	Register	$-\theta_4 t$
cNot	Q4	Q3	
cR_z	Q4	Register	$2n_{34}t$
cNot	Q4	Q3	
cNot	Q4	Q2	
cR_z	Q4	Register	$2n_{24}t$
cNot	Q4	Q2	
cNot	Q4	Q1	
cR_z	Q4	Register	$2n_{14}t$
cNot	Q4	Q1	
cNot	Q3	Q2	
cR_z	Q3	Register	$2n_{23}t$
cNot	Q3	Q2	
cNot	Q3	Q1	
cR_z	Q3	Register	$2n_{13}t$
cNot	Q3	Q1	
cNot	Q2	Q1	
cR_z	Q2	Register	$2n_{12}t$
cNot	Q2	Q1	
Two Electron Operators: excitation-excitation operator			
XXYY			
Hadamard	Q1		
Hadamard	Q2		
R_x	Q3		$-\pi/2$
R_x	Q4		$-\pi/2$
cNot	Q2	Q1	
cNot	Q3	Q2	
cNot	Q4	Q3	
cR_z	Q4	Register	$-t(h_{1423} + h_{1243})/4$
cNot	Q4	Q3	
cNot	Q3	Q2	
cNot	Q2	Q1	
R_x	Q4		$\pi/2$
R_x	Q3		$\pi/2$
Hadamard	Q2		

continued on next page

Gate	Target qubit	Control qubit	Parameter
Hadamard	Q1		
YYXX			
R_x	Q1	-$\pi/2$	
R_x	Q2	-$\pi/2$	
Hadamard	Q3		
Hadamard	Q4		
cNot	Q2	Q1	
cNot	Q3	Q2	
cNot	Q4	Q3	
cR_z	Q4	Register	$-t(h_{1423} + h_{1243})/4$
cNot	Q4	Q3	
cNot	Q3	Q2	
cNot	Q2	Q1	
Hadamard	Q4		
Hadamard	Q3		
R_x	Q2		$\pi/2$
R_x	Q1		$\pi/2$
XYYX			
Hadamard	Q1		
R_x	Q2		-$\pi/2$
R_x	Q3		-$\pi/2$
Hadamard	Q4		
cNot	Q2	Q1	
cNot	Q3	Q2	
cNot	Q4	Q3	
cR_z	Q4	Register	$t(h_{1423} + h_{1243})/4$
cNot	Q4	Q3	
cNot	Q3	Q2	
cNot	Q2	Q1	
Hadamard	Q4		
Hadamard	Q3		
R_x	Q2		$\pi/2$
R_x	Q1		$\pi/2$
YXXY			
R_x	Q1		$\pi/2$
Hadamard	Q2		
Hadamard	Q3		
R_x	Q4		$\pi/2$
cNot	Q2	Q1	
cNot	Q3	Q2	
cNot	Q4	Q3	
cR_z	Q4	Register	$t(h_{1423} + h_{1243})/4$
cNot	Q4	Q3	
cNot	Q3	Q2	
cNot	Q2	Q1	
R_x	Q1		$-\pi/2$
Hadamard	Q2		
Hadamard	Q3		
R_x	Q4		$-\pi/2$

References

[1] A. Szabo and N. Ostlund, *Modern Quantum Chemistry: Introduction to Advanced Electronic Structure Theory* (Dover Publications, Mineola, NY, 1996).
[2] T. Helgaker, P. Jorgensen and J. Olsen, *Molecular Electronic-Structure Theory* (John Wiley and Sons, Chichester, UK, 2000).
[3] C. Sherrill, J. Chem. Phys. **132**, 110902 (2010).
[4] T.D. Ladd, F. Jelezko, R. Laflamme, Y. Nakamura, C. Monroe and J.L. O'Brien, Nature **464**, 45 (2010).
[5] R. Feynman, Optics News (now OPN) **11** (11), 11–22 (1982).
[6] S. Lloyd, Science **273**, 1073 (1996).
[7] A. Aspuru-Guzik, A. Dutoi, P. Love and M. Head-Gordon, Science **309**, 1704 (2005).
[8] D. Lidar and H. Wang, Phys. Rev. E **59**, 2429 (2008).
[9] I. Kassal, S.P. Jordan, P.J. Love, M. Mohseni and A. Aspuru-Guzik, Proc. Natl. Acad. Sci. **105**, 18681 (2008).
[10] G. Ortiz, J. Gubernatis, E. Knill and R. Laflamme, Phys. Rev. A **64**, 022319 (2001).
[11] I. Kassal and A. Aspuru-Guzik, J. Chem. Phys. **131**, 224102 (2009).
[12] I. Kassal, J. Whitfield, A. Perdomo-Ortiz, M.H. Yung and A. Aspuru-Guzik, preprint, arXiv:1007.2648 (2010). <http://arxiv.org/abs/1007.2648>.
[13] B.P. Lanyon, J.D. Whitfield, G.G. Gillet, M.E. Goggin, M.P. Almeida, I. Kassal, J.D. Biamonte, M. Mohseni, B.J. Powell, M. Barbieri, A. Aspuru-Guzik and A.G. White, Nature Chem. **2**, 106 (2010).
[14] J. Du, N. Xu, X. Peng, P. Wang, S. Wu and D. Lu, Phys. Rev. Lett **104**, 030502 (2010).
[15] D. Feller, J. Comp. Chem. **17**, 1571 (1996).
[16] K.L. Schuchardt, B.T. Didier, T. Elsethagen, L. Sun, V. Gurumoorthi, J. Chase, J. Li and T.L. Windus, J. Chem. Inf. Model. **47**, 1042 (2007).
[17] D.P. DiVincenzo, Fortschr. Phys. **48**, 771 (2000), also arXiv:quant-ph/0002077.
[18] M. Nielsen and I. Chuang, *Quantum Computation and Quantum Information* (Cambridge University Press, Cambridge, UK, 2001).
[19] P. Jordan and E. Wigner, Z. Phys. A. **47**, 631 (1928).
[20] R. Somma, G. Ortiz, J.E. Gubernatis, E. Knill and R. Laflamme, Phys. Rev. A **65**, 042323 (2002).
[21] E. Ovrum and M. Hjorth-Jensen, preprint, arXiv:0705.1928 (2007). <http://arxiv.org/abs/0705.1928>.
[22] N. Hatano and M. Suzuki, in *Quantum Annealing and Other Optimization Methods*, edited by A. Das and B.K. Chakrabarti (Springer, Berlin, Germany, 2005), Lectures Notes in Physics, pp. 37–68.
[23] D.W. Berry, G. Ahokas, R. Cleve and B.C. Sanders, Commun. Math. Phys. **270**, 359–371 (2007).
[24] R. Beals, H. Buhrman, R. Cleve, M. Mosca and R. de Wolf, Quantum Lower Bounds by Polynomials. in *Proceedings of FOCS' 98*. <also see, http://arxiv.org/abs/quant-ph/9802049>, pp. 352–361.
[25] S. Parker and M. Plenio, Phys. Rev. Lett. **85**, 3049–52 (2000).
[26] A. Kitaev, preprint, arXiv:quant-ph/9511026 (1995). <http://arxiv.org/abs/quant-ph/9511026>.
[27] A. Tomita and K. Nakamura, Int. J. Quantum Information **2**, 119 (2004).
[28] M. Dobšíček, G. Johansson, V. Shumeiko and G. Wendin, Phys. Rev. A **76**, 030306(R) (2007).
[29] L. Xiu-Mei, L. Jun and S. Xian-Ping, Chinese Phys. Lett. **24**, 3316 (2007).
[30] K.R. Brown, R.J. Clark and I.L. Chuang, Phys. Rev. Lett. **97**, 050504 (2006).
[31] E. Farhi, J. Goldstone, S. Gutmann and M. Sipser, Science **292**, 472 (2000).
[32] L.A. Wu, M.S. Byrd and D.A. Lidar, Phys. Rev. Lett. **89**, 057904 (2002).
[33] A. Perdomo-Ortiz, S.E. Venegas-Andraca and A. Aspuru-Guzik, Quantum Information Processing pp. 1–20 (2010).
[34] S. Boixo, E. Knill and R.D. Somma, Quant. Inf. Comp. **9**, 0833 (2009).
[35] P. Wocjan and A. Abeyesinghe, Phys. Rev. A **78**, 042336 (2008).
[36] J. Kempe, A. Kitaev and O. Regev, SIAM J. Computing **35** (5), 1070–1097 (2006).
[37] R. Oliveira and B. Terhal, Quant. Inf. Comp. **8**, 0900 (2008).
[38] H. Wang, S. Kais, A. Aspuru-Guzik and M. Hoffmann, Phys. Chem. Chem. Phys. **10**, 5388 (2008).
[39] H. Wang, S. Ashhab and F. Nori, Phys. Rev. A **79**, 042335 (2009).
[40] N. Ward, I. Kassal and A. Aspuru-Guzik, J. Chem. Phys. **130**, 194105 (2009).
[41] L. Veis and J. Pittner, preprint, arXiv:1008.3451 (2010). <http://arxiv.org/abs/1008.3451>.
[42] R.P. Muller, Python Quantum Chemistry (PyQuante) program, version 1.6 (Sandia National Laboratories, Albuquerque, NM, 2007).
[43] D. Gottesman, preprint, arXiv:0904.2557 (2009). <http://arxiv.org/abs/0904.2557>.
[44] A.Y. Kitaev, Russian Math. Surveys **52**, 1191 (1997).
[45] C.R. Clark, T.S. Metodi, S.D. Gasster and K.R. Brown, Phys. Rev. A **79**, 062314 (2009).

Table A1. The quantum circuits corresponding to evolution of the listed Hermitian second-quantized operators. Here, p, q, r, and s are orbital indices corresponding to qubits such that the population of state $|1\rangle$ determines the occupancy of the orbitals. It is assumed that the orbital indices satisfy $p > q > r > s$. These circuits were found by performing the Jordan-Wigner transformation given in Eqs. (5b) and (5a) and then propagating the obtained Pauli spin variables [20]. In each circuit, $\theta = \theta(h)$ where h is the integral preceding the operator. Gate $\mathsf{T}(\theta)$ is defined by $\mathsf{T}|0\rangle = |0\rangle$ and $\mathsf{T}|1\rangle = \exp(-i\theta)|1\rangle$, G is the global phase gate given by $\exp(-i\phi)\mathbf{1}$, and the change-of-basis gate Y is defined as $R_x(-\pi/2)$. Gate H refers to the Hadamard gate. For the number-excitation operator, both $\mathsf{M} = \mathsf{Y}$ and $\mathsf{M} = \mathsf{H}$ must be implemented in succession. Similarly, for the double excitation operator each of the 8 quadruplets must be implemented in succession. The global phase gate must be included due to the phase-estimation procedure. Phase estimation requires controlled versions of these operators which can be accomplished by changing all gates with θ-dependence into controlled gates.

Second quantized operators			Circuit
Number operator	$h_{pp}a_p^\dagger a_p$		
Excitation operator	$h_{pq}(a_p^\dagger a_q + a_q^\dagger a_p)$		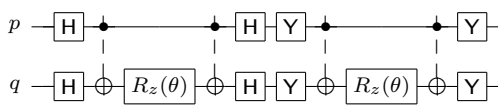
Coulomb and exchange operators	$h_{pqqp}a_p^\dagger a_q^\dagger a_q a_p$		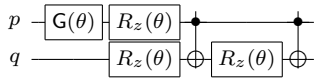
Number-excitation[a] operator	h_{pqqr}	$(a_p^\dagger a_q^\dagger a_q a_r + a_r^\dagger a_q^\dagger a_q a_p)$	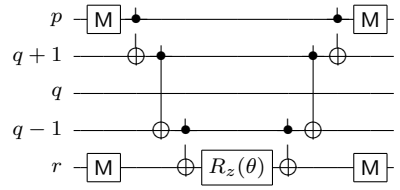 where $\mathsf{M}=\{\mathsf{H},\mathsf{Y}\}$
Double excitation operator	h_{pqrs}	$(a_p^\dagger a_q^\dagger a_r a_s + a_s^\dagger a_r^\dagger a_q a_p)$	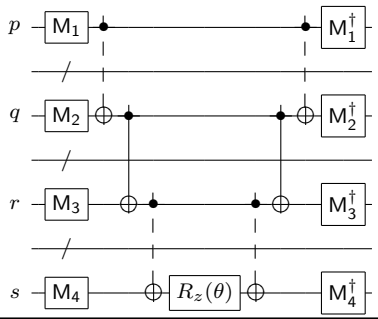 where $(\mathsf{M}_1,\mathsf{M}_2,\mathsf{M}_3,\mathsf{M}_4)=$ $\{$(H,H,H,H), (Y,Y,Y,Y), (H,Y,H,Y),(Y,H,Y,H), (Y,Y,H,H),(H,H,Y,Y), (Y,H,H,Y), (H,Y,Y,H)$\}$
Notation:			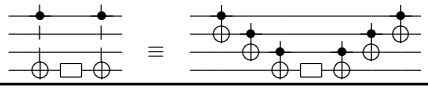

[a]The spin variable representation of this operator depends on whether q lies in the range p to r or outside of it.

Table A2. The spin variable representation of second quantized Hermitian operators after performing the Jordan-Wigner transformation to yield tensor products of Pauli sigma matrices (spin variables) that have the proper anti-commutation relations. See Eqs. (5b) and (5a) for the form of the transformation used. The subscripts label the qubit and the molecular spin orbital that corresponds to that qubit. The pre-factors h_{ij} and h_{ijkl} are one- and two- electron integrals given in Eqs. (3) and (4). In our algorithm, these are calculated using a classical computer. Rarely is this the limiting step since the basis sets are typically chosen for ease of integration. In this table, we provide for the case that the one- and two-electron integrals are complex. The integrals h_{pqqp} and h_{pqpq} are referred to as the Coulomb and exchange integrals, respectively. The exchange operator has the same representation (with opposite sign) as the Coulomb integral due to the commutation relations. The circuit representation of the exponentiation of each of these term is given in Fig. A1.

Description	Second Quantization[a]	Pauli representation
Number Operator	$h_{pp}a_p^\dagger a_p$	$\frac{h_{pp}}{2}(\mathbf{1}_p - \sigma_p^z)$
Excitation Operator	$h_{pq}a_p^\dagger a_q + h_{qp}a_q^\dagger a_p$	$\frac{1}{2}\left(\bigotimes_{k=q+1}^{p-1}\sigma_k^z\right)\begin{pmatrix}\Re\{h_{pq}\}(\sigma_q^x\sigma_p^x+\sigma_q^y\sigma_p^y)\\ +\Im\{h_{pq}\}(\sigma_q^y\sigma_p^x-\sigma_q^x\sigma_p^y)\end{pmatrix}$
Coulomb Operators	$h_{pqqp}a_p^\dagger a_q^\dagger a_q a_p$	$\frac{h_{pqqp}}{4}\left(\mathbf{1}-\sigma_p^z-\sigma_q^z+\sigma_p^z\sigma_q^z\right)$
Number with[b] Excitation Operator	$h_{pqqr}a_p^\dagger a_q^\dagger a_q a_r + h_{rqqp}a_r^\dagger a_q^\dagger a_q a_p$	$\left(\bigotimes_{k=r+1}^{p-1}\sigma_k^z\right)\left[\begin{pmatrix}\Re\{h_{pqqr}\}(\sigma_r^x\sigma_p^x+\sigma_r^y\sigma_p^y)\\ +\Im\{h_{pqqr}\}(\sigma_r^y\sigma_p^x-\sigma_r^x\sigma_p^y)\end{pmatrix} - \sigma_q^z\begin{pmatrix}\Re\{h_{pqqr}\}(\sigma_r^x\sigma_p^x+\sigma_r^y\sigma_p^y)\\ +\Im\{h_{pqqr}\}(\sigma_r^y\sigma_p^x-\sigma_r^x\sigma_p^y)\end{pmatrix}\right]$
Double Excitation Operator	$h_{pqrs}a_p^\dagger a_q^\dagger a_r a_s + h_{srqp}a_s^\dagger a_r^\dagger a_q a_p$	$\left(\bigotimes_{k=s+1}^{r-1}\sigma_k^z\right)\left(\bigotimes_{k=q+1}^{p-1}\sigma_k^z\right)\begin{pmatrix}\frac{\Re\{h_{pqrs}\}}{8}\begin{pmatrix}\sigma_s^x\sigma_r^x\sigma_q^x\sigma_p^x-\sigma_s^x\sigma_r^x\sigma_q^y\sigma_p^y+\sigma_s^x\sigma_r^y\sigma_q^x\sigma_p^y\\ +\sigma_s^y\sigma_r^x\sigma_q^x\sigma_p^y+\sigma_s^y\sigma_r^x\sigma_q^y\sigma_p^x-\sigma_s^y\sigma_r^y\sigma_q^x\sigma_p^x\\ +\sigma_s^x\sigma_r^y\sigma_q^y\sigma_p^x+\sigma_s^y\sigma_r^y\sigma_q^y\sigma_p^y\end{pmatrix}\\ +\frac{\Im\{h_{pqrs}\}}{8}\begin{pmatrix}\sigma_s^y\sigma_r^x\sigma_q^x\sigma_p^x+\sigma_s^x\sigma_r^y\sigma_q^x\sigma_p^x-\sigma_s^x\sigma_r^x\sigma_q^y\sigma_p^x\\ -\sigma_s^x\sigma_r^y\sigma_q^y\sigma_p^y-\sigma_s^y\sigma_r^x\sigma_q^y\sigma_p^y+\sigma_s^y\sigma_r^y\sigma_q^x\sigma_p^y\\ +\sigma_s^y\sigma_r^y\sigma_q^x\sigma_p^y+\sigma_s^y\sigma_r^x\sigma_q^y\sigma_p^x\end{pmatrix}\end{pmatrix}$

[a]It is assumed that $p > q > r > s$ for all cases listed.

[b]The spin variable representation of this operator depends if q is an orbital in the range p to r or if it is outside this range.

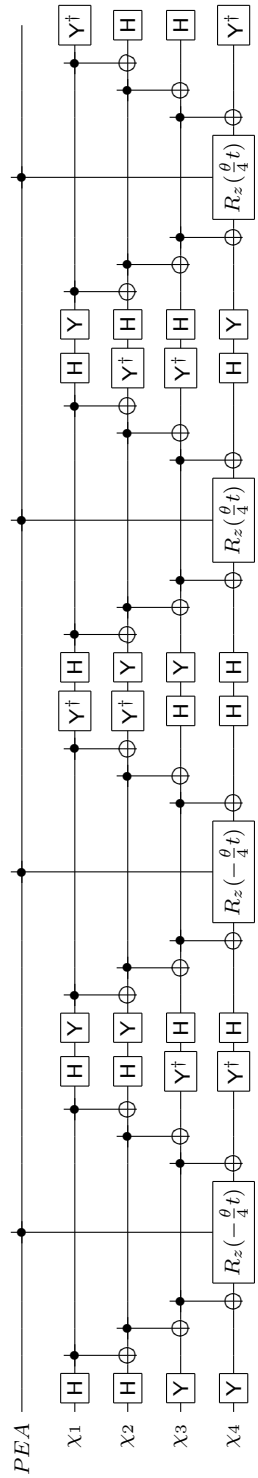

Table A3. A circuit that implements the unitary propagator associated with the two electron operators of the H_2 Hamiltonian in the minimal basis. The circuit is derived from the two non-vanishing real integrals of the two-electron interaction and the corresponding operators. In the circuit, $\theta \equiv h_{1423} + h_{1243} = .36257$. In Eq. 22 two of the four pre-factors vanish due to the spin orthogonality however if all spins are aligned there will be eight terms to simulate.